# Transcriptional regulation of odontogenic ameloblast-associated protein gene by TNF-α and the effect of miR-200b on TNF-α-induced amelotin gene expression

# （TNF-α による ODAM 遺伝子の転写調整と TNF-α 刺激による AMTN 遺伝子発現へのマイクロ RNA-200b の影響）

日本大学大学院松戸歯学研究科歯学専攻

鶴屋　祐人

（指導：小方　賴昌　教授）

## Preface

This article is based on a main manuscript, “Transcriptional regulation of human odontogenic ameloblast-associated protein gene by tumor necrosis factor-α” in the Inflammation Research, and a reference manuscript, “MiR-200b suppresses TNF-α-induced AMTN production in human gingival epithelial cells” in the Odontology.

## Abstract

Amelotin (AMTN) is an enamel protein that is localized in junction epithelium (JE) of gingiva, and odontogenic ameloblast-associated protein (ODAM) is produced by maturation stage ameloblasts and JE. AMTN and ODAM is suggested to be involved in the attachment between JE and tooth enamel. MicroRNA is a small non-coding RNA that regulates gene expression at post-transcriptional level by binding to the 3’-untranslated region (3’-UTR) of target mRNAs. To elucidate transcriptional regulation of human AMTN and ODAM genes in inflamed gingiva, we have analyzed the effects of miR-200b on the expression of AMTN, and analyzed the effects of TNF-α on the expression of ODAM gene in Ca9-22 gingival epithelial cells.

TNF-α (10 ng/ml, 12 h) increased miR-200b expression significantly in Ca9-22 cells. Transfection of miR-200b expression plasmid in Ca9-22 cells significantly increased miR-200b levels in the cells. Total RNAs was extracted from Ca9-22 cells transfected with miR-200b expression plasmid or miR-200b inhibitor and stimulated by TNF-α. TNF-α-induced AMTN mRNA levels were partially inhibited by miR-200b overexpression and enhanced by miR-200b

inhibitor.

Ca9-22 cells were transfected with -353AMTN 3'-UTR LUC constructs and miR200b expression plasmid, and LUC activities were measured with or without stimulation by TNF-α. Total RNAs were extracted from Ca9-22, Sa3 and HSY cells stimulation by TNF-α (10 ng/ml). ODAM mRNA and protein levels were analyzed by qPCR and Western blotting. Luciferase (LUC) analyses were performed using LUC constructs inserted in various lengths of ODAM gene promoter. Gel shift and chromatin immunoprecipitation (ChIP) assays were carried out.

TNF-α increased ODAM mRNA and protein levels at 3 to 24 h. TNF-α induced LUC activities of the ODAM gene promoter constructs, and the activities were inhibited by protein kinase A, tyrosine kinase, MEK1/2, PI3-kinase and NF-κB inhibitors. Gel shift and ChIP assays revealed that TNF-α increased CCAAT/enhancer binding protein (C/EBP) β and Yin Yang1 (YY1) binding to three kinds of C/EBPs and YY1 elements.

These results demonstrate that miR-200b suppresses AMTN gene expression in the human gingival epithelial cells. And TNF-α stimulates ODAM gene transcription via three kinds of C/EBPs and YY1 elements in the human ODAM gene promoter.

## 1. Introduction

Odontogenic ameloblast-associated protein (ODAM) is a secretory protein expressed by maturation stage ameloblasts and junction epithelium (JE), which is a member of secretory

calcium-binding phosphoprotein (SCPP) gene family [1, 2]. In amelogenesis, ODAM is expressed during the maturation stage of ameloblasts and modulates enamel mineralization through the regulation of matrix metalloproteinase-20 (MMP-20), which is one of the proteolytic enzymes found during enamel formation [2-4]. ODAM knockout mice had no dramatic effect on enamel but in older mice, the JE presented some detachment, an increase in inflammation and apical down-growth [5]. ODAM interacts strongly with amelotin (AMTN), which is also expressed in maturation stage ameloblasts and JE, and is involved in enamel mineralization [6]. ODAM promotes JE-related gene expression via activation of WNT1 signaling in ameloblast-like cells, and is able to promote hydroxyapatite nucleation [7, 8].

Amelotin (AMTN) is a secreted enamel protein that was firstly identified as an expression product of ameloblasts in the maturation stage of amelogenesis [9]. The protein is also found at the internal basal lamina of junctional epithelium (JE) [10, 11]. Localization of AMTN suggests that it might play some part in the attachment of JE to tooth surface, and in the maintenance of the integrity of periodontal tissue. Recently, we have reported that AMTN gene transcription was regulated by tumor necrosis factor-α (TNF-α) and interleukin-1β (IL-1β) in human gingival epithelial cells [12, 13]. These results suggest that the expression of AMTN could be regulated in inflammatory conditions.

The reduced enamel epithelium becomes transformed into JE during tooth eruption. JE cells exhibit a rapid turnover and contribute to the equilibrium between the host and bacteria and the rapid repair of gingival injuries such as inflammation and external stimulus [14, 15]. The JE is

an epithelial structure located at the bottom of the gingival sulcus that blocks the supporting tissue of the tooth from constant microbiological challenges. JE is attached to the tooth surface by hemidesmosome and represents the first line of defense against periodontal disease. This incompletely differentiated non-keratinized epithelium is formed by the fusion of reduced enamel organs and oral epithelium [16, 17].

Periodontal disease contributes significantly to the global burden of oral diseases and shares common risk factors with several chronic diseases [18, 19]. Periodontitis is caused by certain periodontopathic bacteria, and immune responses to the bacterial products such as lipopolysaccharide and proteolytic enzymes, followed by the production of inflammatory cytokines causes periodontal tissue destruction [20-22].

In chronic inflammatory diseases, the increased production of matrix metalloproteinase and prostaglandins from monocytes and fibroblasts induces the production of inflammatory cytokines such as IL and TNF. TNF-α is a cytokine which plays an important role in both acute and chronic inflammatory responses in several diseases such as postmenopausal osteoporosis, rheumatoid arthritis (RA), and periodontitis [23, 24].

MicroRNAs (miRNAs) are small, non-cording RNAs that repress gene expressions by hybridization to target transcripts. Many kinds of miRNAs have been discovered in the human genome and each miRNA has the potential to repress the expression of various mRNAs [25-28]. Active miRNAs function as post-transcriptional regulators through base-pairing interactions between the seed region of them with complementary sequences in the 3'-

untranslated regions (3'-UTR) of the target mRNAs [28]. MiRNA mediated suppression of gene expression is thought to occur by inhibiting translation and promoting mRNA degradation [29]. miRNA functions are diverse and related to biological processes, such as development, differentiation, cell proliferation, inflammation, and apoptosis. Several studies have demonstrated that various kinds of miRNAs are closely associated with different processes of periodontitis, which is an inflammatory reaction of periodontal tissue [30-32]. We have previously reported that miRNA expression in inflamed and non-inflamed gingiva from Japanese patients and three most overexpressed miRNAs in inflamed gingiva were miR-150, miR-223, and miR-200b [33]. In addition, we have reported that miR-223 and miR200b regulate the production of inflammatory cytokines in human gingival fibroblasts [34, 35]. MiR-200b is one of the miR-200 family which also includes miR-200a, miR-200c, miR-141 and miR-429. It has been reported that miR-200 family members except miR-429 were selectively expressed in the epithelial cells and indicated the association with epithelial to mesenchymal transition [36, 37].

To elucidate the transcriptional regulation of ODAM gene and role of ODAM in inflamed gingiva, we have analyzed the effect of TNF-α on human ODAM gene expression using human gingival epithelial Ca9-22 cells. And to determine the effects of miR-200b on the AMTN gene expression in human gingival epithelial cells, we transfected miR-200b expression plasmid or miR-200b inhibitor in Ca9-22 human gingival epithelial cells and analyzed the AMTN gene expressions.

## 2. Materials and Methods

### Reagents

Fetal calf serum (FCS), lipofectamine 2000, penicillin and streptomycin, and Tryp$^{TM}$LE Express were purchased from Invitrogen (Carlsbad, CA). PGL3-basic vector, pSV-β-galactosidase (β-Gal) control vector and mitogen-activated protein (MAP) kinase kinase (MEK1/2) inhibitor U0126 were obtained from Promega (Madison, WI). Protein kinase C (PKC) inhibitor H7 was from Seikagaku Corporation (Tokyo, Japan). Protein kinase A (PKA) inhibitor KT5720, IMD0354 [inhibitor of kappa-B kinase β (IKKβ) inhibitor], complete protease inhibitor cocktail, and phenylmethylsulfonyl fluoride (PMSF) were purchased from Sigma-Aldrich Japan (Tokyo, Japan). LY249002 [phosphatidylinositol 3-kinase (PI3-K) inhibitor] was from Calbiochem (San Diego, CA, USA). Triptolide [nuclear factor-kappa B (NF-κB) inhibitor] was from Tocris Bioscience (Bristol, UK). BMS345541 [selective allosteric inhibitor of IKK ($IC_{50}$ values are 0.3 and 4.0 μM for IKKβ and IKKα respectively] was from Abcam (Cambridge, UK). Alpha-minimum essential medium (α-MEM), Dulbecco's Modified Eagle Medium (DMEM), tyrosine kinase inhibitor herbimycin A (HA), and human recombinant TNF-α were purchased from Wako (Tokyo, Japan). ISOGEN II was purchased from Nippon Gene (Tokyo, Japan). Radioimmunoprecipitaion (RIPA) lysis buffer was purchased from Santa Cruz Biotechnology (Dallas, TX, USA). PrimeScript RT reagent kit and SYBR Premix Ex Taq II were purchased from Takara-Bio (Tokyo, Japan). ECL prime Western Blotting Detection Reagents were purchased from GE Healthcare (Buckinghamshire, UK). All chemicals used

were analytical grade. The Mir-X miRNA First-Strand Synthesis Kit and SYBR Advantage qPCR Premix were purchased from Clontech (Mountain View, CA, USA). Expression plasmid for miRNA (pEZX-MR04) was obtained from GeneCopoeia (Rockville, MD, USA). miRCURY LNA inhibitor and miRCURY LNA inhibitor Control were purchased from Exiqon (Woburn, MA, USA). All chemicals used were analytical grade.

**Cell cultures**

Human gingival epithelial Ca9-22 cells and human parotid gland adenocarcinoma HSY cells or human gingival squamous cell carcinoma-derived Sa3 cells were cultured in α-MEM or DMEM supplemented with 10% FCS at 37°C in 5% $CO_2$ and 95% air. The cells were seeded in 60 mm cell culture dishes, grown to confluence, and then cultured in serum-free α-MEM for 12 h. Ca9-22 cells were then stimulated with various concentrations of TNF-α (0.1, 1, 10, and 50 ng/ml) for 12 h or 10 ng/ml TNF-α for 3, 6, 12, and 24 h (0 h as a control). Twenty-four hours after plating, Ca9-22 cells at 60-80% confluence were transfected with the control plasmid (pEZX-MR04; 3 μg), miRExpress precursor miRNA expression plasmid for miR-200b (3 μg), miRCURY LNA Inhibitor Control (5 nM), or miRCURY LNA Inhibitor for miR-200b (5 nM) using lipofectamine 2000. Two days following transfection, the cells were cultured in α-MEM without serum for 12 h, and then stimulated with TNF-α (10 ng/ml) for 12 h prior to harvest.

**Real-time polymerase chain reaction (PCR)**

Total RNA was extracted using ISOGEN II and analyzed for the expression of ODAM and glyceraldehyde 3-phosphate dehydrogenase (GAPDH) mRNAs. Total RNA (1 μg) was used as a template for cDNA which was prepared using the PrimeScript RT reagent kit. Quantitative real-time PCR was performed using the following primer sets: AMTN forward, 5'-GTTGAATGTACAACAGCAACTGCAC-3'; AMTN reverse, 5'-TTCCAT CCTGGACATCTGGATTA-3', Human ODAM forward, 5'-ATGGTCCTACCCTGGGAACAA-3'; Human ODAM reverse, 5'-ACAGCAATTTCAGGAGCTGTG-3'; GAPDH forward, 5'-GCACC GTCAAGGCTGAGAAC-3'; GAPDH reverse, 5'-ATGGTGGTGAGACGCCAGT-3'; using the SYBR Premix Ex Taq II in a TP950 Thermal Cycler Dice Real-Time System (Takara-Bio). The amplification reactions included 2x SYBR Premix EX Taq (12.5 μl), 0.4 μM forward and reverse primers (0.2 μl), and 70 ng cDNA (7 μl) for AMTN and ODAM, and 50 ng cDNA (5 μl) for GAPDH, the final volume was 25 μl. To reduce variability between replicates, PCR premixes containing all reagents except for cDNA were prepared and aliquoted into 0.2 ml PCR tubes (NIPPON Genetics, Tokyo, Japan). The thermal cycling condition was 30 seconds at 95°C, 45 cycles of 5 sec at 95°C and 30 sec at 60°C. Post-PCR melting curves confirmed the specificity of single-target amplification, and the expressions of AMTN and ODAM relative to the GAPDH were performed three times.

For the analysis of miRNA expression levels, cDNA was synthesized using the Mir-X miRNA

First-Strand Synthesis kit. Quantitative real-time PCR was performed using the following primer sets: mir-200b forward, 5'-TAATAC TGCCTGGTAATGATGA-3'; mRQ 3' reverse primer, U6 forward primer, U6 reverse primer including Mir-X miRNA First-Strand Synthesis Kit using SYBR Advantage qPCR Premix in TP800 thermal cycler dice real-time system (TakaraBio, Tokyo, Japan). The amplification reactions were performed in 25 μl of the final reaction mixture containing 2 × SYBR Advantage qPCR Premix (12.5 μl), 10 μM forward and reverse primers (1 μl), and 2 ng cDNA (10 μl) for miR-200b and 1 ng cDNA (5 μl) for U6. The expressions of miR-200b relative to U6, and AMTN relative to GAPDH were determined in triplicated.

**Western blotting**

Total proteins extracted from Ca9-22 cells using the RIPA lysis buffer were separated by 12% sodium dodecyl sulfate-polyacrylamide gel electrophoresis (SDS-PAGE) and transferred to a Hybond 0.2 μm PVDF membrane. The membrane was blocked with 3% skim milk for 30 min at room temperature (RT), and incubated overnight with anti-ODAM (PA5-100656; Invitrogen, Carlsbad, CA, USA) and anti-αTubulin (sc-5286; Santa Cruz Biotechnology) antibodies. Anti-rabbit and anti-mouse IgG conjugated with horseradish peroxidase (HRP) were used as the secondary antibodies. Immune response was detected by ECL prime Western blotting detection reagent.

**Immunofluorescence**

Eight chamber slides were coated with 10 μg/ml fibronectin at 37°C for 30 min. Ca9-22 cells were plated on 8-chamber slides of 10,000 cells/ml and cultured in α-MEM containing 10% FCS for 12 h. After exchanging the α-MEM for serum-free for 6 h, the cells were treated with 10 ng/ml TNF-α for 6 h. After 6 h, cells were fixed with 4% paraformaldehyde for 10 min and treated with 0.1% Triton X-100 for 5 min for permeabilization. Cells were blocked with 2.5% goat serum in 4% bovine serum albumin for 20 min at RT. Primary antibody was rabbit polyclonal anti-ODAM (16509-1-AP; Proteintech) used at 1:200 for 2 h at 37°C. Secondary antibodies were Alexa Fluor® 488 goat anti-rabbit IgG used at 1:200 for 1 h at RT. Coverslips were mounted with Antifade Poly/Mount with DAPI (Polysciences, Warrington, PA, USA). For analysis of the expression of ODAM by Ca9-22 cells, cells were imaged using a LSM 5 EXCITER (Carl Zeiss Microscopy, Jena, Germany). Exposure time and intensity range were the same for each image. Contrast-adjusted post imaging was equal for all images.

**Luciferase assays**

Three different regions [locating at exon 9; 1-88 (from the beginning of exon 9 to the 88th base of 3'-UTR), 83-707 and 708-1692] in the 3'-UTR of human AMTN gene, including predicted miR-200b binding sites, were amplified from human genomic DNA by PCR and subsequently cloned into XbaI site downstream of the luciferase (LUC) gene of -353AMTN construct (AMTN 3'-UTR (exon 9; 1-88) LUC, AMTN 3'-UTR (83-707) LUC, and AMTN 3'-UTR

(708-1692) LUC) [6]. The transfection mixture included the control plasmid (1 μg) or the miR-200b expression plasmid (1 μg), 3'-UTR AMTN LUC constructs (1 μg), and β-Gal plasmid (1 μg) as a transfection control.

To explore the TNF-α response regions in human ODAM gene promoter, we prepared luciferase (LUC) constructs by ligating human ODAM gene promoters into pGL3-basic vector. Various lengths of human ODAM gene promoter sequences (-85ODAM: -85 to +60; -116ODAM: -116 to +60; -174ODAM: -174 to +60; -200ODAM: -200 to +60; -300ODAM: -300 to +60; -330ODAM: -330 to +60; -480ODAM: -480 to +60; -750ODAM: -750 to +60; -950ODAM: -950 to +60) were prepared by PCR amplification, and these DNAs were cloned into the Sac I site of the pGL3-basic multi cloning site. After 24 h plating, Ca9-22 cells at 60-80% confluence were transfected by transfection mixture including 1 μg LUC construct and 1 μg β-Gal plasmid as an internal control using lipofectamine 2000. At 48 h after transfection, the cells were deprived of serum for 12 h, TNF-α (10 ng /ml) was added for 12 h prior to harvesting. The LUC assays were performed according to the supplier's protocol (PicaGene; Toyo Ink, Tokyo, Japan) using a luminescence reader (AB-2270 Luminescencer Octa; ATTO, Tokyo, Japan) to measure LUC activities. Eight kinds of protein kinase inhibitors were used to inhibit protein kinases. Forty-eight h after transfection, the cells were deprived of serum for 12 h, and first treated with H7 (5 μM), KT5720 (100 nM), LY294002 (10 μM), BMS345541 (4 μM), IMD0354 (5 μM), triptolide (100 nM) and U0126 (5 μM) for 30 min, or HA (1 μM) for 4 h, then stimulated with TNF-α (10 ng/ml) for 12 h before harvesting the cells.

**Gel mobility shift assays**

Nuclear extracts were prepared using confluent Ca9-22 cells. They were cultured in serum-free α-MEM for 12 h and then stimulated with TNF-α (10 ng/ml) for 0 (control), 3, 6, and 12 h in α-MEM without serum. Double-stranded oligonucleotides encompassing the CCAAT/enhancer binding protein (C/EBP1), Yin Yang 1 (YY1), C/EBP2, GATA, activator protein 1 (AP1) and C/EBP3 in the human ODAM gene promoter were used as DNA probes containing 5'-Cy5 (Sigma-Aldrich Japan). 5'-Cy5-labeled oligonucleotide and complementary oligonucleotide were annealed under optimal conditions (50 mM Tris-HCl pH 7.9, 10 mM $MgCl_2$). Nuclear proteins (4 μg) were incubated for 20 min at RT with 2 pM Cy5-labeled double-stranded oligonucleotide in the binding buffer containing 50 mM KCl, 0.5 mM EDTA, 10 mM Tris-HCl (pH 7.9), 1 mM dithiothreitol, 0.04 % Nonidet P-40, 5% glycerol, and 1 μg of poly dI-dC. After incubation, the DNA-protein complexes were separated by 6% nondenaturing acrylamide gels run at 200 V. After electrophoresis, the gels were analyzed using Typhoon TRIO + variable mode imager (GE Healthcare) and ChemiDoc (BIO RAD). The double-stranded oligonucleotide sequences were: C/EBP1 forward; 5'-CCTGGTCCTTTTTGAACAATGATTGGTCC-3', C/EBP1 reverse; 5'-CGGACCAATCATTGTTCAAAAAGGACCAG-3', YY1 forward; 5'-CTATTAGCTAAGCCATTGTCTGAAACCCAC-3', YY1 reverse; 5'-CGTGGGTTTCAGACAATGGCTTAGCTAATA-3', C/EBP2 forward; 5'-CATTACTAAAAGTGTGGGAATCCATATAC-3', C/EBP2 reverse; 5'-

CGTATATGGATTCCCACACTTTTAGTAAT-3', C/EBP3 forward; 5'-CAGTATCCAGTTTTATTCAATTAGAGTATC-3', C/EBP3 reverse; 5'-CGATACTCTAATTGAATAAAACTGGATACT-3'.

**Chromatin immunoprecipitation (ChIP) assays**

To examine whether C/EBPβ and YY1 transcription factors are able to interact directly with human ODAM gene promoter and how TNF-α regulates these transcription factors interactions with the C/EBP1, C/EBP2, C/EBP3 and YY1 we performed ChIP assays. Confluent Ca9-22 cells in 100 mm culture dishes were stimulated with TNF-α (10 ng/ml) for 0, 3, 6, 12, and 24 h, then the cells were fixed with 160 µl of formaldehyde for 10 min to cross-link the DNA-protein complexes. The fixed cells were rinsed twice by a wash buffer (1 mM PMSF and complete protease inhibitor cocktail in the PBS [-]) on ice, collected by scrape, and centrifuged for 5 min at 4°C. After the cells were resuspended by an SDS buffer (1% SDS, 0.01 M EDTA, 0.05 M Tris-HCl, pH 8.1), lysate was sonicated to shear the protein-fragmentary DNA complexes. Sonicated cell supernatants were diluted in a 10-fold ChIP dilution buffer (0.01% SDS, 1.1% Triton X-100, 1.2 mM EDTA, 16.7 mM Tris-HCl, pH 8.9, 16.7 mM NaCl, 1 mM PMSF, and complete protease inhibitor cocktail in $H_2O$). The diluted supernatants were assigned as a control which included non-specific protein-DNA complexes and precleared with 80 µl Protein A/G plus Agarose (25% slurry) for 30 min at 4°C with gentle agitation. For the immunoprecipitation of protein-DNA complexes, 2 µg of rabbit polyclonal anti-YY1 antibody

(ab38422, Abcam, Cambridge, UK), anti-C/EBPβ (SAB4500112, Sigma-Aldrich, Inc.), and the appropriate unconjugated normal rabbit anti-IgG antibody (SC-2027, Santa Cruz, Biotechnology, Inc.) were used for 300 µl of precleared supernatant and incubated overnight at 4°C with constant rotation. 60 µl of Protein A/G plus Agarose (25% slurry) was added for 1 h at 4°C with rotation to collect the antibody/histone complexes and pellet agarose by gentle centrifugation (1,000 rpm for 1 min). After removing the supernatant that contained unbound chromatin, the pellet was washed twice with 1 ml each of Low Salt buffer (0.1% SDS, 1% Triton X-100, 2 mM EDTA, 20 mM Tris-HCl, pH 8.1, 150 mM NaCl in $H_2O$), High Salt buffer (0.1% SDS, 1% Triton X-100, 2 mM EDTA, 20 mM Tris-HCl, pH 8.1, 500 mM NaCl in $H_2O$), lithium chloride (LiCl) buffer (0.25 M LiCl, 0.1% NP-40, 1% deoxycholate, 0.5 mM EDTA, 0.01 M Tris-HCl, pH 8.1 in $H_2O$), and 1 ml of Tris and EDTA (TE) buffer (10 mM Tris-HCl, pH 8.1, 1 mM EDTA in $H_2O$). After the TE buffer had been removed, Protein A/G plus Agarose/antibody/chromatin complexes were resuspended in 250 µl of elution buffer (1% SDS and 0.1 M $NaHCO_3$ in $H_2O$) and incubated at RT for 15 min with gentle rotation. After spin-down of the agarose beads, 20 µl of 5 M NaCl was added to the supernatant for reverse cross-linking, and 10 µl 0.5 M EDTA, 20 µl 1 M Tris-HCl, pH 6.5, and 1 µl 10 mg/ml proteinase K were added to the degradate of the antibodies and proteins. DNA was recovered by phenol/chloroform/isoamylalcohol extraction and ethanol precipitation. The purified DNA was subjected to PCR amplification (1 cycle, 94°C for 2 min; amplification was performed for 30-37 cycles, denatured at 94°C, 30 sec; 53 or 55°C, 30 sec; 68°C, 1 min; and final extension was

at 68°C, 1 min) for the C/EBP1, CEBP2, C/EBP3 and YY1 sites within the human ODAM promoter using C/EBP1 ChIP forward; 5'-ACCCACTGAATCACTGGTCC-3', C/EBP1 ChIP reverse; 5'-CTACTGCTTGGCACTTCTCT-3', C/EBP2 ChIP forward; 5'-ACAGGAAAACATTTCTCAGG-3', C/EBP2 ChIP reverse; 5'-CTAATAACCTCTTTCCTAAT-3', C/EBP3 ChIP forward; GACTTTATTAAAGATATTAA-3', C/EBP3 ChIP reverse; ATAATTCTATTCTACTCTTT-3', YY1 ChIP forward; 5'-ATATACCACCTAAATGATTA-3', YY1 ChIP reverse; 5'-AAGGACCAGTGATTCAGTGG-3' primers. Quick Tag HS Dye Mix was utilized for the PCR procedure, and the PCR products were separated on 2% agarose gels and visualized with ultraviolet light.

**MiRNA target analysis**

Potential miR-200b target sites involved in AMTN gene expression were identified using TargetScan 7.1 [38], miRanda (August 2010 release) [39], and miRBase 21 [40]. TargetScan predicts biological targets of miRNAs according to matches with the 7-8 bp seed region, surrounding context, and the degree of conservation across species [38]. miRanda incorporates the probability of mRNA downregulation using a regression model trained on sequence context features of miRNA duplex [39]. All animal miRNA sequences from the miRBase Sequence database are scanned against 3'-UTRs predicted from all available species, and P-values based on statistical models are assigned to individual miRNA target binding sites, multiple sites in a single UTR, and sites that appear to be conserved in multiple species [40].

**Statistical analysis**

Triplicate samples were analyzed for each experiment. The significance of differences between r1control and treatment groups was determined using the one-way ANOVA and multiple comparison calibration (Tukey–Kramer method).

## 3. Results

**MiR-200b expression in human gingival epithelial cells**

We previously reported that the miR-200b expression was increased in inflamed gingiva using miRNA microarray [16]. To elucidate the effect of TNF-α on the expression of miR-200b in Ca9-22 cells, we performed real-time PCR. TNF-α (10 ng/ml, 12 h) increased miR-200b expression significantly in Ca9-22 cells (Fig. 1A). Transfection of miR-200b expression plasmid in Ca9-22 cells significantly increased miR-200b levels in the cells (Fig. 1B).

**Decreasing of AMTN mRNA by miR-200b expression**

To determine whether the AMTN mRNA expression is regulated by miR-200b, Ca9-22 cells were transfected with miR-200b expression plasmid and stimulated with TNF-α (10 ng/ml) for 12 h. TNF-α induced AMTN mRNA levels in Ca9-22 cells and the induction was decreased by transfection of miR-200b expression plasmid (Fig. 2A). Next, we evaluated the effect of miR-200b inhibitor on TNF-α-induced AMTN mRNA level. MiR-200b inhibitor further increased

TNF-α-induced AMTN mRNA levels in Ca9-22 cells (Fig. 2B). AMTN mRNA levels in Ca9-22 cells not treated with TNF-α was decreased by miR-200b overexpression plasmid and was increased by miR-220b inhibitor, but there are no significant differences (Fig. 2A, B).

**Luciferase assays of human AMTN 3'-UTR constructs**

To analyze whether miR-200b can bind to the 3'-UTR of human AMTN mRNA and regulate human AMTN expression, we made 3 kinds of human AMTN 3'-UTR LUC constructs which were inserted different 3'-UTR regions containing miR-200b target sites of the human AMTN gene (Fig. 3A). Three kinds of human AMTN 3'-UTR (exon9; 1-88, 83-707, and 708-1692) LUC constructs and control plasmid or miR-200b expression plasmid were transfected in Ca9-22 cells, and stimulated with TNF-α (10 ng/ml, 12 h). Transcriptional activities of these 3 constructs were increased by TNF-α and partially suppressed by miR-200b overexpression. The basal activity of 708-1692 construct was significantly suppressed by miR-200b (Fig. 3B).

**Effect of TNF-α on ODAM mRNA and protein levels in Ca9-22**

To study the regulation of ODAM gene transcription by TNF-α, we performed real-time PCR using total RNAs obtained from Ca9-22, Sa3 and HSY cells. The dose-response relation of ODAM mRNA levels after stimulation by TNF-α was established by treating Ca9-22 cells with different concentrations of TNF-α for 12 h. ODAM mRNA levels were significantly increased by 0.1, 1, 10 and 50 ng/ml TNF-α, and reached maximum by 10 ng/ml TNF-α (Fig. 4A). Then,

10 ng/ml TNF-α was used to study the time-course effect on ODAM mRNA expressions. TNF-α (10 ng/ml) induced ODAM mRNA levels significantly at 3, 6, 12 and 24 h in Ca9-22, Sa3 and HSY cells, respectively (Fig. 4B-D). ODAM protein levels were increased with TNF-α (10 ng/ml) at 3, 6, and 12 h and reached maximum at 24 h. α-Tubulin was used as control (Fig. 5).

Immunofluorescence of the expression of ODAM in Ca9-22 cells was increased after stimulation by TNF-α (10 ng/ml) for 12 h, compared with Ca9-22 cells without treatment by TNF-α. Nuclei and ODAM were stained with DAPI (blue) and anti-ODAM antibody via a secondary antibody bound to Alexa Fluor® 488 (green). Nuclei and ODAM expressions in the cells appeared in the merged image (×100). Differential interference contrast (DIC) was used for gaining proper images of unstained cells (Fig. 6).

**Luciferase assays of ODAM promoter constructs**

Promoter sequence that is unique to the human ODAM gene between -1 to -480 contains three kinds of C/EBPs (C/EBP1; nts -59 to -72, C/EBP2; nts -144 to -160 and C/EBP3; nts -304 to -317), a YY1 (nts -93 to -109), a GATA (nts -175 to -184), an AP1 (nts -228 to -238) elements (Fig. 7). Subsequent studies were performed to find the response elements of TNF-α regulated transcription in the 5'-flanking region of the human ODAM gene, various-sized human ODAM gene promoter DNAs ligated to a LUC plasmid were transiently transfected into Ca9-22 cells and their transcriptional activities were measured in the presence and absence of TNF-α. The

LUC activities of -85ODAM, -116ODAM, -174ODAM, -200ODAM, -300ODAM, -330ODAM, -480ODAM, - 700ODAM and -950ODAM were increased after 12 h treatment with TNF-α (10 ng/ml; Fig. 5). TNF-α-induced LUC activities of -330ODAM, -174ODAM and -116ODAM were significantly higher than the TNF-α-induced LUC activities of -300ODAM, -116ODAM and -85ODAM (Fig. 8). We next investigated the effects of PKC inhibitor H7, PKA inhibitor KT5720, tyrosine kinase inhibitor HA, MEK1/2 inhibitor U0126, PI3-K inhibitor LY294002, IKKβ and IKKα inhibitor BMS345541, IKKβ inhibitor IMD0354 and NF-κB inhibitor triptolide on the transcriptional activities of -480ODAM in the presence and absence of TNF-α. Whereas TNF-α induced luciferase activities were inhibited by KT5720, HA, U0126, LY294002, BMS345541, IMD0354 and triptolide, H7 could not inhibit TNF-α induced -480 ODAM activity (Fig. 9).

**Gel shift assays**

To determine the nuclear proteins binding to C/EBP1, YY1, C/EBP2 and CEBP3 elements, and mediate the effects of TNF-α on the ODAM gene transcription, Cy5-labeled double-stranded oligonucleotides were incubated with nuclear proteins (4 μg) extracted from Ca9-22 cells that were either not treated (Control) or treated with TNF-α (10 ng/ml) for 3, 6, and 12 h. After stimulation by TNF-α, C/EBP1, YY1, C/EBP2 and C/EBP3-protein complexes were increased at 3 and 6 h and reached maximum at 12 h (Fig. 10). When we used GATA and AP1 as probes, DNA-protein complexes could not be induced by TNF-α (data not shown). These DNA-protein

complexes represent how specific interactions were confirmed by competition experiments in a 40-fold molar excess of non-labeled C/EBP1, YY1, C/EBP2 and C/EBP3 reduced DNA-protein complexes formations (Fig. 11, lanes 3, 9, 15, and 21). C/EBP1, C/EBP2, C/EBP3 and YY1 oligonucleotides disrupted C/EBP1 (Fig. 11, lanes 3-6), YY1 (Fig. 11, lanes 9-12) and C/EBP3-protein complexes formations (Fig. 11, lanes 21-24), respectively. However, C/EBP1 oligonucleotide could not disrupted the formation of C/EBP2-protein complexes, suggesting the constituents of C/EBP1- and C/EBP2-binding proteins are not the same (Fig. 11, lane 16). These results demonstrate that the nuclear proteins binding to C/EBP1, C/EBP2, C/EBP3 and YY1 elements are similar transcription factors. Antibodies to C/EBPβ and YY1 were used to further characterize the proteins in the complexes formed by C/EBP1, C/EBP2, C/EBP3 and YY1. The addition of C/EBPβ antibody partially disrupted the formations of the C/EBP1, C/EBP2, C/EBP3-protein complexes (Fig. 12, lanes 4, 12 and 16). Anti-YY1 antibody almost completely disrupted the formation of the YY1-protein complexes (Fig. 12, lane 8).

**ChIP assays**

We performed ChIP assays to examine whether C/EBPβ and YY1 transcription factors are able to interact with C/EBP1, C/EBP2, C/EBP3 and YY1 elements in the human ODAM gene promoter *in vivo*. TNF-α induced C/EBPβ binding to C/EBP1, C/EBP2 and C/EBP3 at 3 to 24 h, and YY1 binding to YY1 at 6 and 12 h. The fragmented DNA-protein complexes were used as positive control (Input) without using the antibodies (Fig. 13). Next, we used PKC inhibitor

(H7), PKA inhibitor (KT5720), tyrosine kinase inhibitor (HA), MEK1/2 inhibitor (U0126) and PI3K inhibitor (LY294002) for ChIP assays to confirm the results of LUC assays using the kinase inhibitors with or without TNF-α treatment. C/EBPβ and YY1 bindings to C/EBP1, C/EBP2, C/EBP3 and YY1 were completely inhibited by HA, U0126, and LY294002, and partially inhibited by KT5720 (Fig. 14).

## 4. Discussion

In this study, we demonstrated that TNF-α increased miR-200b expression in Ca9-22 cells (Fig. 1A). This result supports our previous report that miR-200b was highly expressed in inflamed gingiva [33], and it is suggested that miR-200b is expressed associated with inflammation in gingival epithelial cells. TNF-α-induced AMTN mRNA levels were partially suppressed by miR-200b in Ca9-22 cells (Fig. 2A), and miR-200b inhibitor further promoted the increase of AMTN mRNA levels induced by TNF-α (Fig. 2B). These findings suggest that AMTN production could be regulated by both TNF-α and miR-200b. We have previously reported that TNF-α-regulated human AMTN gene transcription was mediated through NF-κB pathway [12]. NF-κB is one of the important nuclear factors which regulate various biological processes, such as cell proliferation, immune responses, and inflammation. NF-κB signaling is divided into two pathways, the canonical and the non-canonical pathways [41].

In the second study, we first demonstrated that human ODAM gene transcription was

increased by TNF-α in human gingival epithelial cells at the mRNA and protein levels (Fig. 4 and 5). In the previous study, we have shown that ODAM, AMTN, IL-1α, IL-1β and IL-6 gene expressions were increased in the inflamed gingiva from patients with chronic periodontitis using DNA microarray [42]. The expression pattern of ODAM and AMTN at the JE were changed during inflammation process [43]. Therefore, the results in this study support those findings at the cellular level.

Inflammatory cytokines such as TNF-α, IL-1β and IL-6 are soluble proteins that bind to specific receptors and induce intracellular signaling cascades. They play a fundamental role in inflammation including periodontal disease [23, 24, and 35]. TNF-α is a typical inflammatory cytokine in the inflamed tissues and induces insulin resistance [44]. Adipocytes express high levels of TNF-α, and TNF-α serum levels are increased in obese, type 2 diabetes and cancer patients [44, 45]. Periodontitis is an inflammatory disease caused by oral bacteria around the gingival sulci, and severe periodontitis can result in destruction of periodontium, alveolar bone resorption and tooth loss [46]. TNF receptor type 1 (TNFR1) and receptor activator of NF-κB ligand (RANKL) are co-expressed in the JE. TNF-α induced RANKL expression is mediated through the TNFR1 and PKA signaling pathways [47].

As the results of LUC assays, transcriptional activity reached maximum via TNF-α in the -330ODAM in which the ODAM gene promoter sequence from +60 to -330 base pairs upstream from the transcription start site was inserted (Fig. 8). These results suggest that there are several transcription factor binding sites which respond to TNF-α in the ODAM gene promoter

sequence up to -330 base pairs upstream (Fig. 7 and 8). NF-κB and C/EBPβ are involved in the regulation of expression of many genes that function in inflammation and immunity [48]. C/EBPs are consist of leucine zipper transcription factor family involved in the regulation of various aspects of cellular differentiation and function in a variety of tissues [49]. C/EBPβ was originally identified as a mediator of IL-6 signaling, binding to IL-6 response elements in the promoters of acute-phase response genes TNF, IL-8 and granulocyte-colony stimulating factor. TNF-α promotes nuclear localization of C/EBPβ in response to inflammatory stress [50]. YY1 is known to have a fundamental role in normal biologic processes such as differentiation, replication, proliferation and embryogenesis [51]. YY1 plays a critical role in promoting IL-6 transcription in RA, which contributes to the inflammation of RA via stimulation of Th17 differentiation [52]. There are three kinds of C/EBP (C/EBP1, C/EBP2 and C/EBP3) and YY1 elements in the human ODAM gene promoter sequence up to -330 base pairs upstream from the transcriptional start site (Fig. 7). In this study, we have shown that C/EBP1, C/EBP2, C/EBP3 and YY1 elements in the human ODAM gene promoter and C/EBPβ and YY1 transcription factors might play important roles in transcriptional regulation of human ODAM gene by TNF-α. Results of LUC, gel mobility shift and ChIP assays indicated that TNF-α induced human ODAM transcription through C/EBPβ and YY1 target C/EBP1, YY1, C/EBP2, and C/EBP3 in the human ODAM gene promoter. The tyrosine kinase inhibitor HA, MEK1/2 inhibitor U0126, PI3-K inhibitor LY294002, IKKβ and IKKα inhibitor BMS345541, IKKβ inhibitor IMD0354 and NF-κB inhibitor triptolide completely inhibited, and the PKA inhibitor

KT5720 partially inhibited the effect of TNF-α on ODAM transcription. From the above results, it was shown that human ODAM gene expression increases during inflammation in human gingival epithelial cells via tyrosine kinases, MEK1/2, PI3-K, PKA and NF-κB signaling pathways.

These results suggest that miR-200b suppressed TNF-α-induced AMTN gene expression in human gingival epithelial cells. ODAM could be increased by inflamed condition in JE and have some physiologically important role in the inflamed periodontal tissue. It was considered that the expression of the ODAM gene in JE is altered by inflammatory cytokines and play crucial role in resistance to inflammation of periodontal tissues.

## 5. References


1. Kawasaki K. The SCPP gene family and the complexity of hard tissues in vertebrates. Cells Tissues Organs. 2011;194(2-4): 108-112.
2. Moffatt P, Smith CE, St-Arnaud R, Nanci A. Characterization of Apin, a secreted protein highly expressed in tooth-associated epithelia. J Cell Biochem. 2008;103(3): 941-956.
3. Park J-C, Park J-T, Son -H-H, Kim H-J, Jeong M-J, Lee C-S, Dey R, Cho M-L. The amyloid protein Apin is highly expressed during enamel mineralization and maturation in rat incisors. Eur J Oral Sci. 2007;115(2): 153-160.
4. Lee H-K, Lee D-S, Ryoo H-M, Park J-T, Park S-J, Bae H-S, Cho M-I, Park J-C. The odontogenic ameloblast-associated protein (ODAM) cooperates with RUNX2 and modulates enamel mineralization via regulation of MMP-20. J Cell Biochem. 2010;111(3): 755-767.
5. Wazen RM, Moffatt P, Ponce KJ, Kuroda S, Nishio C, Nanci A. Inactivation of the Odontogenic ameloblast-associated gene affects the integrity of the junctional epithelium and gingival healing. Eur Cell Mater. 2015;30: 187-199.
6. Holcroft J, Ganss B. Identification of amelotin- and ODAM-interacting enamel matrix proteins using the yeast two-hybrid system. Eur J Oral Sci. 2011;119 Suppl 1:301-306.
7. Song D, Yang S, Tan T, Wang R, Ma Z, Wang Y, Wang L. ODAM promotes junctional epithelium-related gene expression via activation of WNT1 signaling pathway in an ameloblast-like cell line ALC. J Periodontal Res. 2021;56: 482-491.

8. Ikeda Y, Neshatian M, Holcroft J, Ganss B. The enamel protein ODAM promotes mineralization in a collagen matrix. Connect Tissue Res. 2018;59: 62-66.

9. Iwasaki K, Bajenova E, Somogyi-Ganss E, Miller M, Nguyen V, Nourkeyhani H, Gao Y, Wendel M, Ganss B. Amelotin a novel secreted, ameloblast-specific protein. J Dent Res. 2005;84: 1127-32.

10. Somogyi-Ganss E, Nakayama Y, Iwasaki K, Nakano Y, Stolf D, McKee MD, Ganss B. Comparative temporospatial expression profling of murine amelotin protein during amelogenesis. Cells Tissues Organs. 2012;195: 535-49.

11. Mofatt P, Smith CE, St-Arnaud R, Simmons D, Wright JT, Nanci A. Cloning of rat amelotin and localization of the protein to the basal lamina of maturation stage ameloblasts and junctional epithelium. Biochem J. 2006;399: 37-46.

12. Yamazaki M, Iwai Y, Noda K, Matsui S, Kato A, Takai H, Nakayama Y, Ogata Y. Tumor necrosis factor-α stimulates human amelotin gene transcription in gingival epithelial cells. Inflamm Res. 2018;67: 351-61.

13. Yamazaki M, Mezawa M, Noda K, Iwai Y, Matsui S, Takai H, Nakayama Y, Ogata Y. Transcriptional regulation of human amelotin gene by interleukin-1β. FEBS Open Bio. 2018;8: 974-85.

14. Schroeder HE, Listgarten MA. The gingival tissues: the architecture of periodontal protection. Periodontol 2000. 1997;13: 91-120.

15. Bosshardt DD, Lang NP. The junctional epithelium: from health to disease. J Dent Res.

2005;84: 9-20.

16. Hormia M, Owaribe K, Virtanen I. The dento-epithelial junction: cell adhesion by type I hemidesmosomes in the absence of a true basal lamina. J Periodontol. 2001;72: 788-797.
17. Schroeder HE, Listgarten MA. The junctional epithelium: from strength to defense. J Dent Res. 2003;82: 158-161.
18. Petersen PE, Ogawa H. Strengthening the prevention of periodontal disease: the WHO approach. J Periodontol. 2005;76: 2187-2193.
19. Petersen PE, Ogawa H. The global burden of periodontal disease: towards integration with chronic disease prevention and control. Periodontol 2000. 2012;60: 15-39.
20. Seymour GJ, Gemmell E, Reinhardt RA, Eastcott J, Taubman MA. Immunopathogenesis of chronic inflammatory periodontal disease: cellular and molecular mechanisms. J Periodontal Res. 1993;28: 478-486.
21. Kato A, Imai K, Ochiai K, Ogata Y. Higher prevalence of Epstein-Barr virus DNA in deeper periodontal pockets of chronic periodontitis in Japanese patients. PLoS One. 2013;8: e71990.
22. Netea MG, van Deuren M, Kullberg BJ, Cavaillon JM, Van der Meer JW. Does the shape of lipid A determine the interaction of LPS with Toll-like receptors? Trends Immunol. 2002;23: 135-139.
23. Faizuddin M, Bharathi SH, Rohini NV. Estimation of interleukin-1beta levels in the gingival crevicular fluid in health and in inflammatory periodontal disease. J Periodontal

Res. 2003;38: 111-114.

24. Mundy GR. Osteoporosis and inflammation. Nutr Rev. 2007; 65(12 Pt 2), S147-S151.

25. Baek D, Villén J, Shin C, Camargo FD, Gygi SP, Bartel DP. The impact of microRNAs on protein output. Nature. 2008;455: 64-71.

26. Grosshans H, Filipowicz W. Molecular biology: the expanding world of small RNAs. Nature. 2008;451: 414-6.

27. Lewis BP, Burge CB, Bartel DP. Conserved seed pairing, often flanked by adenosines, indicates that thousands of human genes are microRNA targets. Cell. 2005;120: 15-20.

28. Shyu AB, Wilkinson MF, van Hoof A. Messenger RNA regulation: to translate or to degrade. EMBO J. 2008;27: 471-81.

29. Guo H, Ingolia NT, Weissman JS, Bartel DP. Mammalian microRNAs predominantly act to decrease target mRNA levels. Nature. 2010;466: 835-40.

30. Priyanka V, Teena K, Vamsi L, Suresh RR, Selvaraj R, Samyukta H, Vettriselvi V. Differential expression of microRNAs let-7a, miR-125b, miR-100 and miR-21 and interaction with NF-kB pathway genes in periodontitis pathogenesis. J Cell Physiol. 2018;233: 5877-84.

31. Irwandi RA, Vacharaksa A. The role of microRNA in periodontal tissue: a review of the literature. Arch Oral Biol. 2016;72: 66-74.

32. Park MH, Park E, Kim HJ, Na HS, Chung J. Porphyromonas gingivalis-induced miR-132 regulates TNFα expression in THP-1 derived macrophages. Springerplus. 2016;5: 761.

33. Ogata Y, Matsui S, Kato A, Zhou L, Nakayama Y, Takai H. MicroRNA expression in inflamed and noninflamed gingival tissues from Japanese patients. J Oral Sci. 2014;56: 253-60.

34. Matsui S, Ogata Y. Effects of miR-223 on expression of IL-1β and IL-6 in human gingival fibroblasts. J Oral Sci. 2016;58: 101-8.

35. Matsui S, Zhou L, Nakayama Y, Mezawa M, Kato A, Suzuki N, Tanabe N, Nakayama T, Suzuki Y, Kamio N, Takai H, Ogata Y. MiR-200b attenuates IL-6 production through IKKβ and ZEB1 in human gingival fibroblasts. Inflamm Res. 2018;67: 965-73.

36. Park SM, Gaur AB, Lengyel E, Peter ME. The miR-200 family determines the epithelial phenotype of cancer cells by targeting the E-cadherin repressors ZEB1 and ZEB2. Genes Dev. 2008;22: 894-907.

37. Wiklund ED, Gao S, Hulf T, Sibbritt T, Nair S, Costea DE, Villadsen SB, Bakholdt V, Bramsen JB, Sørensen JA, Krogdahl A, Clark SJ, Kjems J. MicroRNA alterations and associated aberrant DNA methylation patterns across multiple sample types in oral squamous cell carcinoma. PLoS ONE. 2011;6: e27840.

38. Grimson A, Farh KK, Johnston WK, Garrett-Engele P, Lim LP, Bartel DP. MicroRNA targeting specificity in mammals: determinants beyond seed pairing. Mol Cell. 2007;27: 91-105.

39. Betel D, Wilson M, Gabow A, Marks DS, Sander C. The microRNA. org resource targets and expression. Nucleic Acids Res. 2008;36: D149-D153153.

40. Kozomara A, Grifths-Jones S. miRBase: integrating microRNA annotation and deep-sequencing data. Nucleic Acids Res. 2011;39: D152-D157157.

41. Hayden MS, Ghosh S. Signaling to NF-kappaB. Genes Dev. 2004;18: 2195-224.

42. Nakayama Y, Takai H, Matsui S, Matsumura H, Liming Zhou, Kato A, Bernhard Ganss, Ogata Y. Proinflammatory cytokines induce amelotin transcription in human gingival fibroblasts. J Oral Sci. 2014;56, 261-268.

43. Nakayama Y, Kobayashi R, Matsui S, Matsumura H, Iwai Y, Noda K, Yamazaki M, Kurita-Ochiai T, Yoshimura A, Shinomura T, Ganss B, Ogata Y. Localization and expression pattern of amelotin, odontogenic ameloblast-associated protein and follicular dendritic cell-secreted protein in the junctional epithelium of inflamed gingiva. Odontology. 2017;105, 329-337.

44. Uysal K T, Wiesbrock S M, Marino M W, Hotamisligil G S. Protection from obesity-induced insulin resistance in mice lacking TNF-alpha function. Nature. 1997;389, 610-614.

45. Katsuki A, Sumida Y, Murashima S, Murata K, Takarada Y, Ito K, Fujii M, Tsuchihashi K, Goto H, Nakatani K, Yano Y. Serum levels of tumor necrosis factor-alpha are increased in obese patients with noninsulin-dependent diabetes mellitus. Journal of Clinical Endocrinology and Metabolism. 1998;83, 859-862.

46. Kato A, Imai K, Ochiai K, Ogata Y. Prevalence and quantitative analysis of Epstein–Barr virus DNA and Porphyromonas gingivalis associated with Japanese chronic periodontitis patients. Clinical Oral Investigations. 2015;19, 1605-1610.

47. Fujihara R, Usui M, Yamamoto G, Nishii K, Tsukamoto Y, Okamatsu Y, Sato T, Asou Y, Nakashima K, Yamamoto M. Tumor necrosis factor-α enhances RANKL expression in gingival epithelial cells via protein kinase A signaling. J Periodontal Res. 2014;49, 508-517.

48. Cappello C, Zwergal A, Kanclerski S, Haas SC, Kandemir JD, Huber R, Page S, Brand K. C/EBPbeta enhances NF-kappaB associated signaling by reducing the level of IkappaB-alpha. Cell Signal. 2009;21, 1918-1924.

49. Lekstrom-Himes J, Xanthopoulos KG. Biological role of the CCAAT/enhancer-binding protein family of transcription factors. J Biol Chem. 1998;273, 28545-28548.

50. Poli V. The role of C/EBP isoforms in the control of inflammatory and native immunity functions. J Biol Chem. 1998;273, 29279-29282.

51. Gordon S, Akopyan G, Garban H, Bonavida B. Transcription factor YY1: structure, function, and therapeutic implications in cancer biology. Oncogene. 2006;25, 1125-1142.

52. Lin J, He Y, Chen J, Zeng Z, Yang B, Ou Q. A critical role of transcription factor YY1 in rheumatoid arthritis by regulation of interleukin-6. J Autoimmun. 2017;77, 67-75.

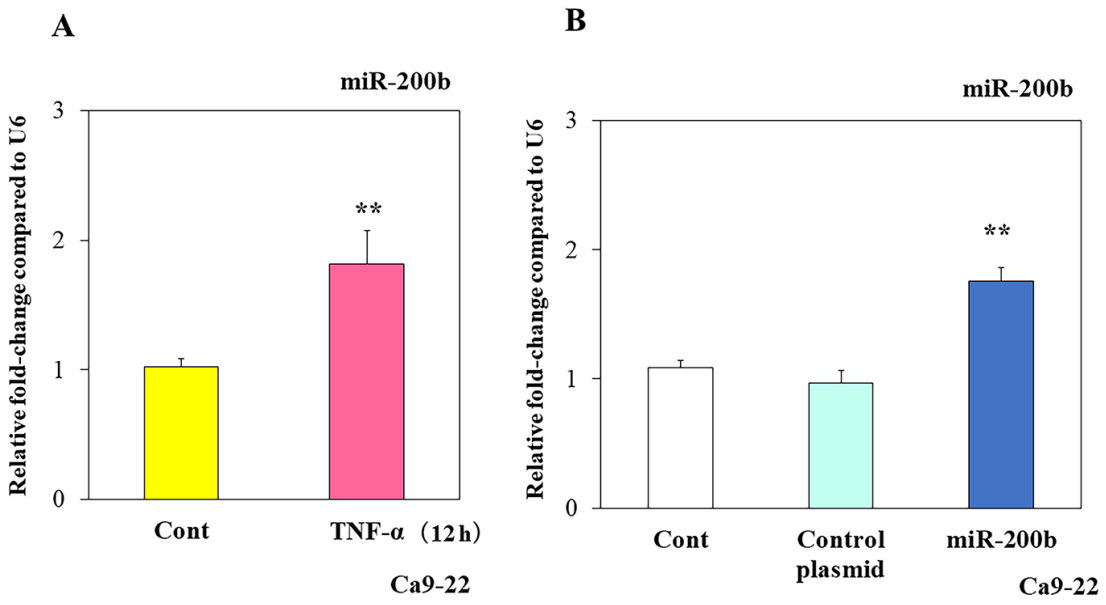


**Fig. 1** Effects of TNF-α and miR-200b expression plasmid on miR-200b mRNA levels in Ca9-22 cells. **A**: Ca9-22 cells were treated with or without TNF-α (10 ng/ml) for 12 h. **B**: Ca9-22 cells were transfected with control plasmid or miR200b expression plasmid for 12 h. miR-200b and U6 mRNA levels were measured by real-time PCR. The experiments were performed in triplicate for each data point. Quantitative analyses of the data sets are shown with standard errors (SE). Significantly different from control; $^{**}P<0.01$

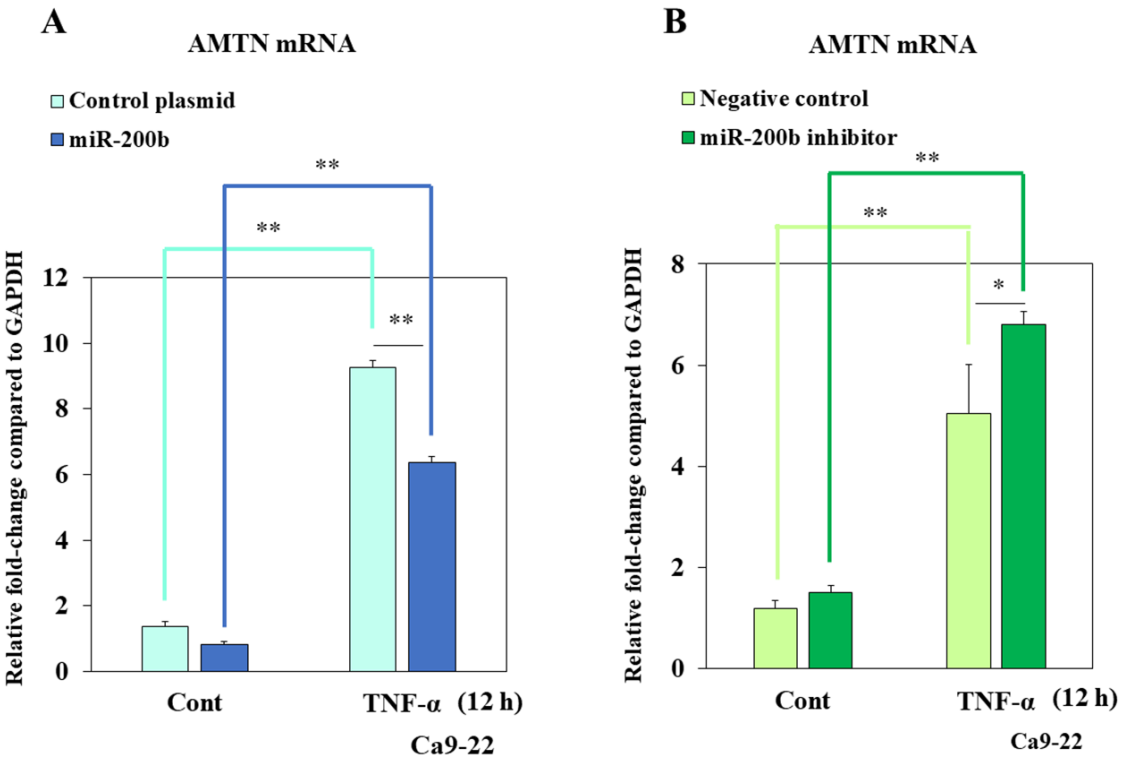


**Fig. 2** Effects of TNF-α and miR-200b expression plasmid or miR-200b inhibitor on AMTN mRNA levels in Ca9-22 cells. **A**: Ca9-22 cells were treated with or without TNF-α (10 ng/ml) for 12 h, and transfected with control plasmid or miR-200b expression plasmid. **B**: Ca9-22 cells were treated with or without TNF-α (10 ng/ml) for 12 h, and transfected with miRCURY LNA Inhibitor Control (5 nM) or miRCURY LNA miR-200b Inhibitor (5 nM). AMTN and GAPDH mRNA levels were measured by real-time PCR. The experiments were performed in triplicate for each data point. Quantitative analyses of the data sets are shown with SE. Significantly different from control; $*P < 0.05$, $**P < 0.01$

A

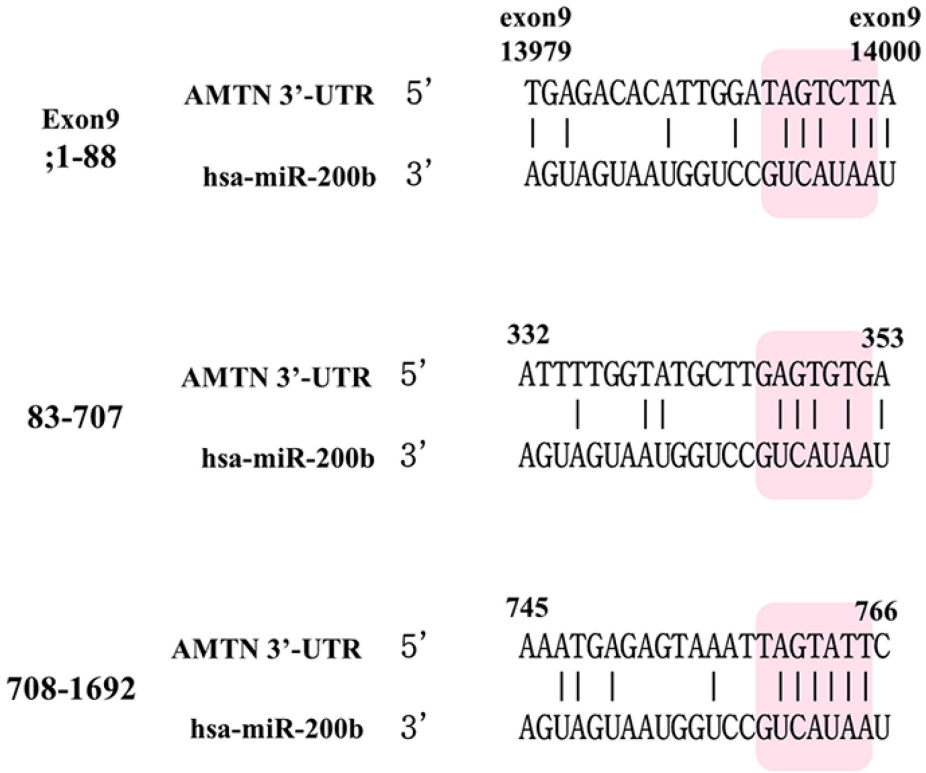
exon9
13979
exon9
14000
Exon9
;1-88
AMTN 3'-UTR 5'
TGAGACACATTGGATAGTCTTA
hsa-miR-200b 3'
AGUAGUAAUGGUCCGUCAUAAU
332
353
83-707
AMTN 3'-UTR 5'
ATTTTGGTATGCTTGAGTGTGA
hsa-miR-200b 3'
AGUAGUAAUGGUCCGUCAUAAU
745
766
708-1692
AMTN 3'-UTR 5'
AAATGAGAGTAAATTAGTATTC
hsa-miR-200b 3'
AGUAGUAAUGGUCCGUCAUAAU

B

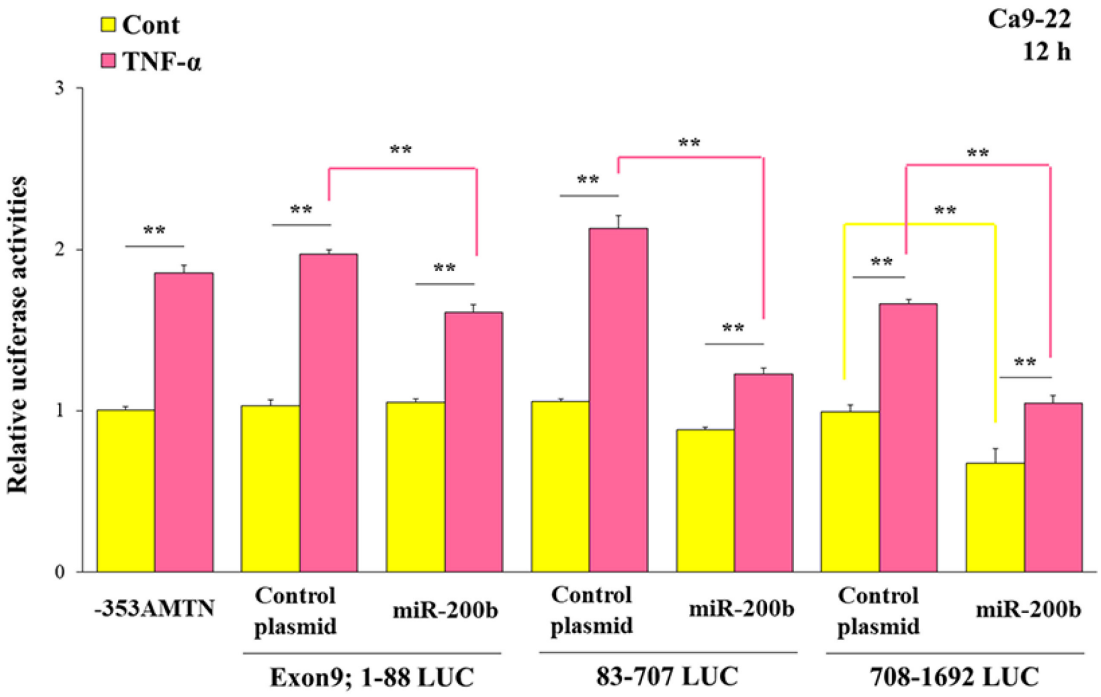
Cont
TNF-α
Ca9-22
12 h
Relative uciferase activities
3
2
1
0
**
-353AMTN
Control plasmid
miR-200b
Exon9; 1-88 LUC
83-707 LUC
708-1692 LUC

**Fig. 3** MiR-200b targets AMTN. **A**: miRanda, miRBase 21 and TargetScan Human (7.1) showed that AMTN 3'-UTR contains several putative miR200b target sites. **B**: TNF-α upregulates human -353AMTN (-353~+60) gene promoter activities. Transcriptional activities of 3 kinds of human AMTN 3'-UTR (exon9; 1-88, 83-707, and 708-1692) LUC constructs were increased by TNF-α (10 ng/ml, 12 h) and partially suppressed by miR-200b overexpression. The basal activity of human AMTN 3'-UTR 708-1692 construct was significantly suppressed by miR-200b in Ca9-22 cells. The results of transcriptional activities obtained from three separate transfections with constructs. Quantitative analyses of the data sets are shown with SE. Significantly different from control; $^{**}P < 0.01$

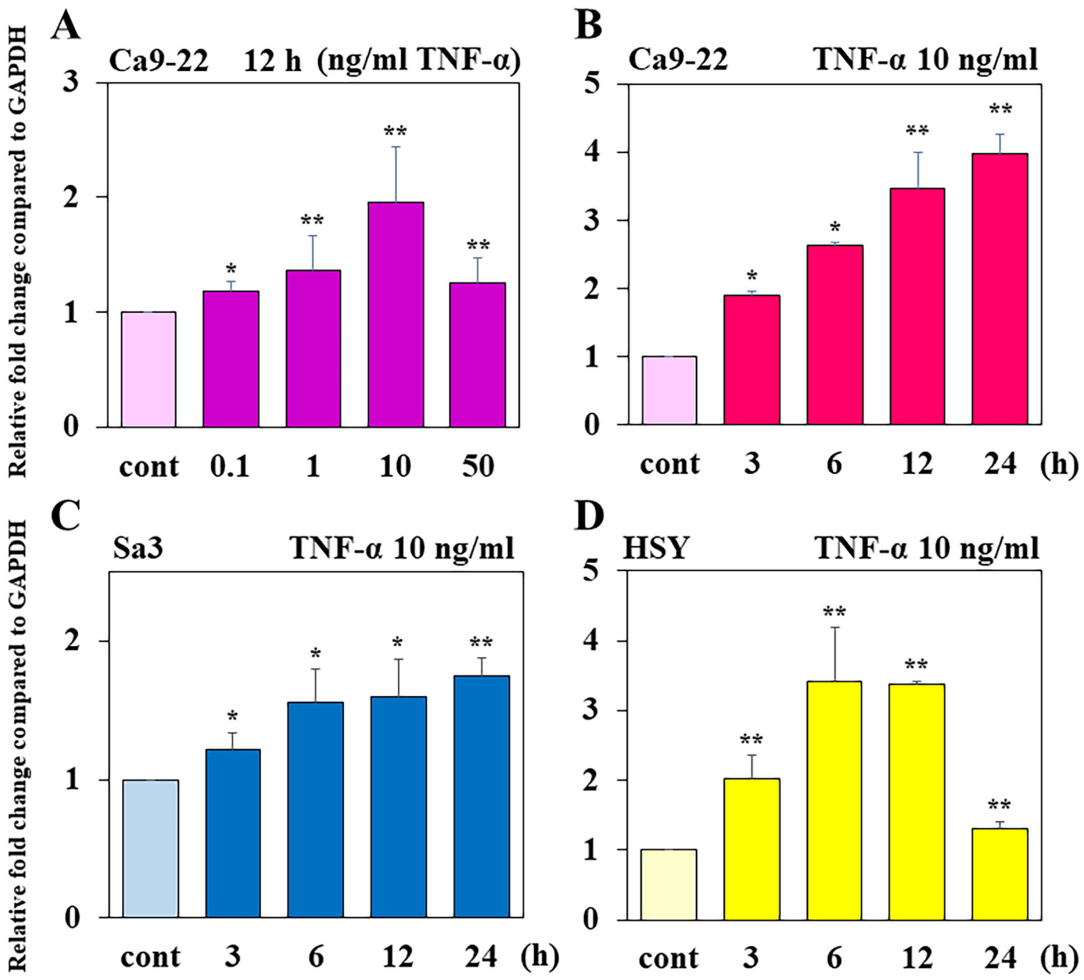


**Fig. 4** Effects of TNF-α on ODAM mRNA levels in Ca9-22, Sa3 and HSY cells. **A**: Dose response effects of TNF-α on ODAM mRNA levels in Ca9-22 cells treated for 12 h. **B**: Ca9-22 cells were treated with TNF-α (10 ng/ml) for 3, 6, 12, and 24 h. **C:** Sa3 cells were treated with TNF-α (10 ng/ml) for 3, 6, 12, and 24 h. **D:** HSY cells were treated with TNF-α (10 ng/ml) for 3, 6, 12, and 24 h. ODAM and GAPDH mRNA levels were analyzed by real-time PCR. The experiments were performed in triplicate for each data point. Quantitative analyses of the data sets are shown with SE. Significantly different from control: $*P < 0.05$, $**P < 0.01$

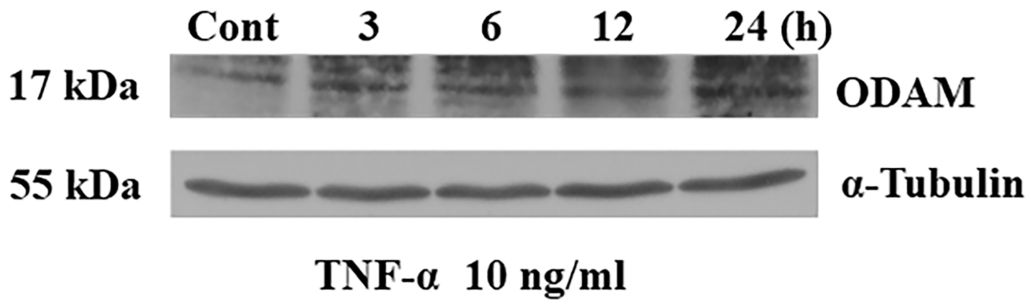


**Fig. 5** Effects of TNF-α on ODAM protein levels in Ca9-22 cells. ODAM protein levels in Ca9-22 cells were analyzed by Western blotting using anti-ODAM (17 kDa) and anti-α-tubulin (55 kDa) antibodies.

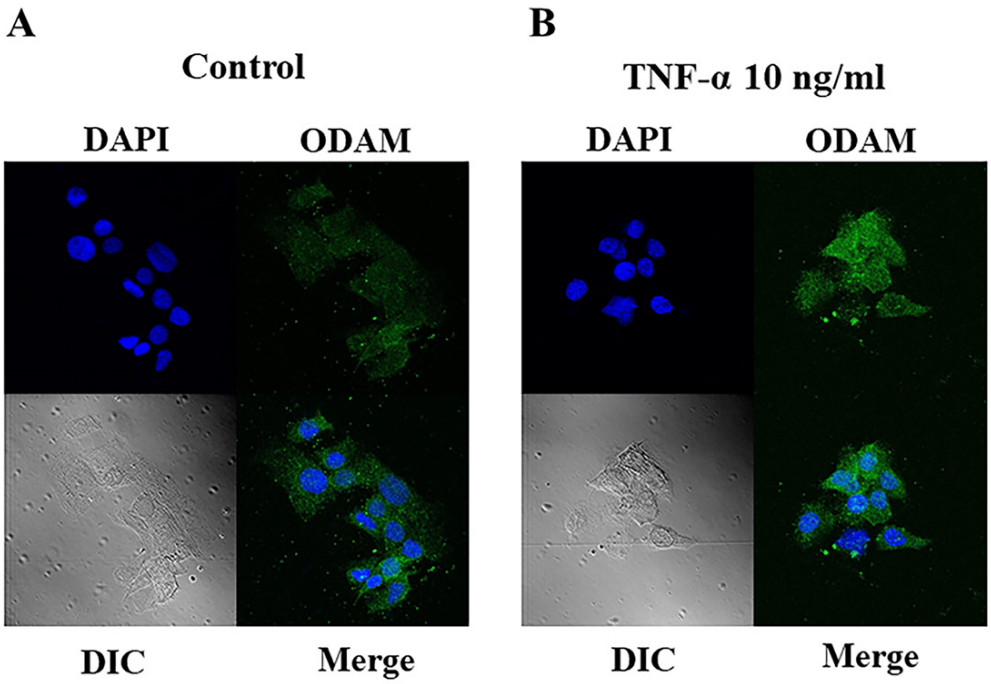


**Fig. 6** Immunofluorescence of ODAM expression in Ca9-22 cells. After culturing Ca9-22 cells in α-MEM containing 10% FCS and converting to serum-free α-MEM for 6 h, the cells (A; control) were treated with 10 ng/ml TNF-α (B) for 12 h. Nuclei and ODAM were stained with

DAPI (blue) and anti-ODAM antibody through immunofluorescence via a secondary antibody bound to Alexa Fluor 488 (green). Nuclei and ODAM expression in Ca9-22 cells appeared in the merged image (9100). DIC was used for gaining proper images of unstained cells.

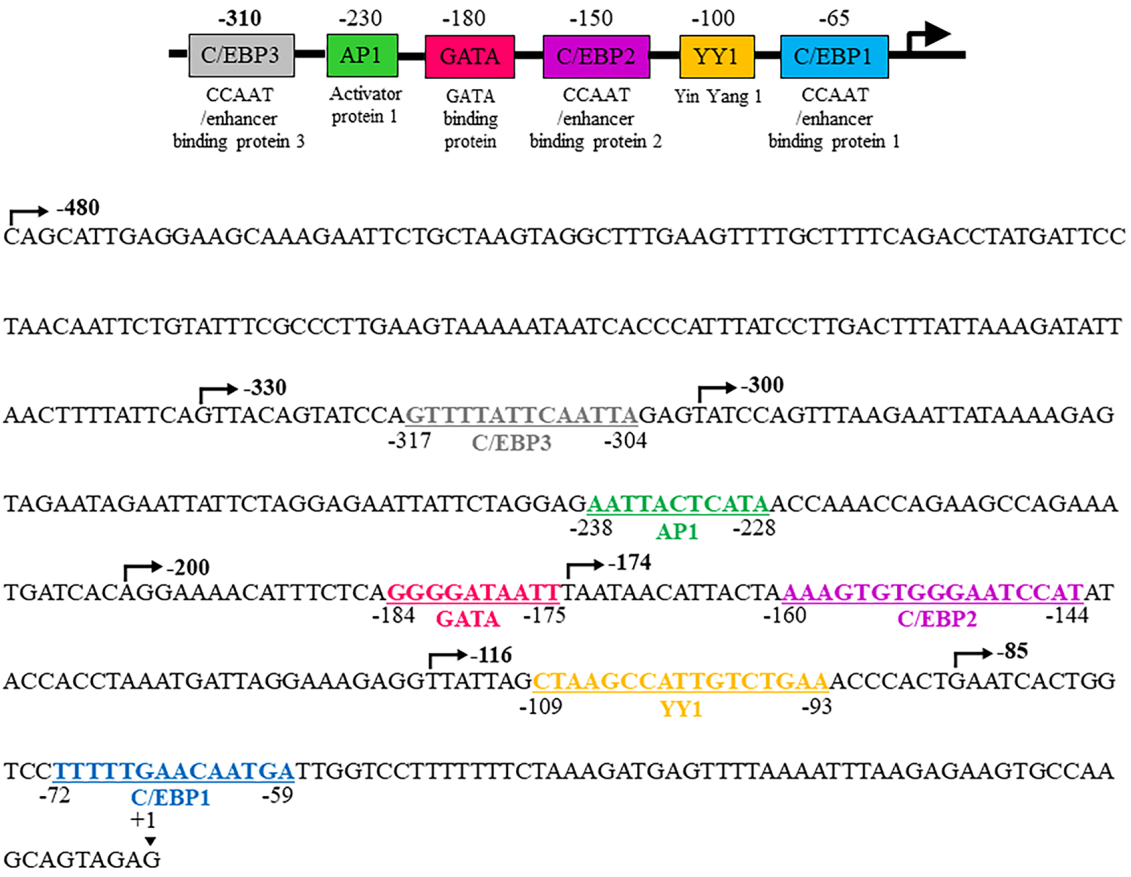


**Fig. 7** Regulatory elements in the proximal promoter of the human ODAM gene. Upper panel: The schematic diagram of human ODAM gene proximal promoter. Lower panel: The nucleotide sequences of the human ODAM gene promoter encompassing an inverted C/EBP1, YY1, C/EBP2, GATA, AP1 and C/EBP3 are shown from -480 to transcription start site (+1).

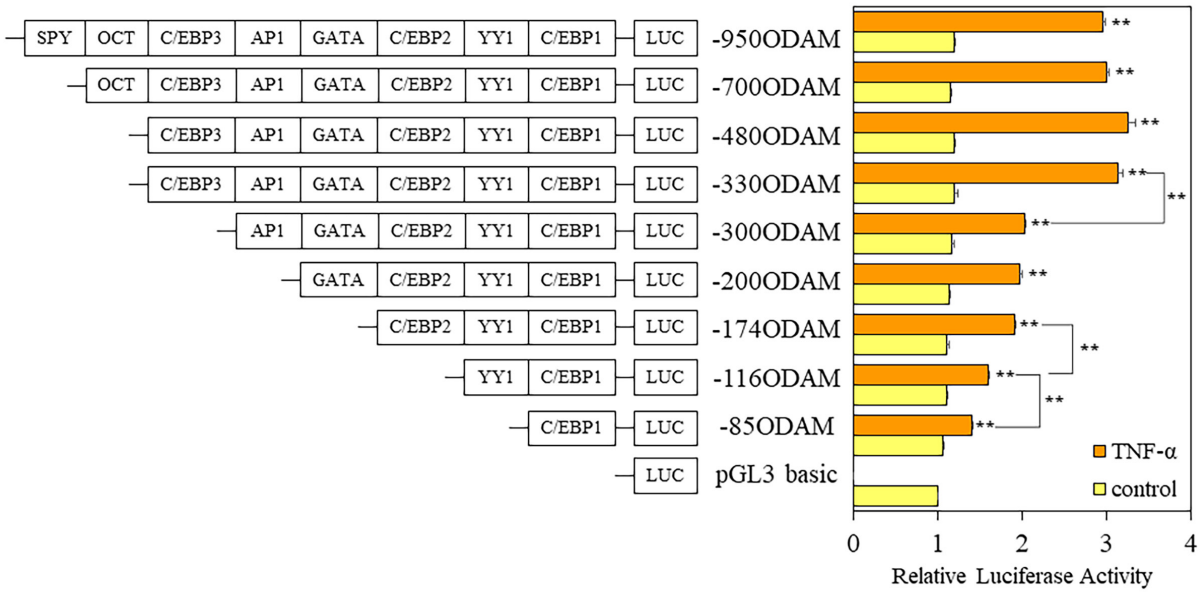


**Fig. 8** TNF-α upregulated human ODAM gene promoter activities. The transcriptional activities of -85ODAM (-85 to +60), -116ODAM (-116 to +60), -174ODAM (-174 to +60), -200ODAM (-200 to +60), -300ODAM (-300 to +60), -330ODAM (-330 to +60), -480ODAM (-480 to +60), -750ODAM (-750 to +60) and -950ODAM (-950 to +60) were increased by TNF-α (10 ng/ml, 12 h) in Ca9-22 cells. The transcriptional activities determined from four separate transfections have been combined, and the values are expressed with SE. Significant differences from control: $^{**}P < 0.01$

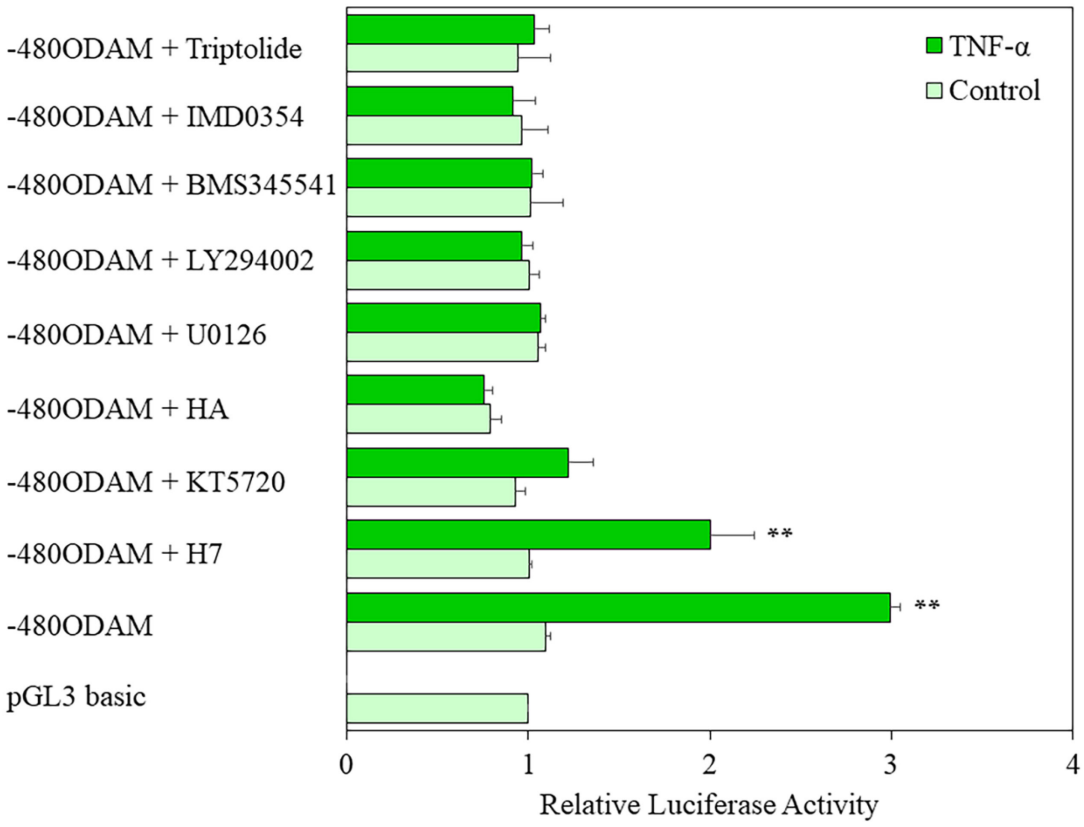


**Fig. 9** Effects of kinase inhibitors on transcriptional activation by TNF-α. TNF-α-induced -480ODAM activities were inhibited by PKA inhibitor (KT5720), tyrosine kinase inhibitor (HA), MEK1/2 inhibitor (U0126), PI3-K inhibitor (LY294002), IKKβ and α inhibitor (BMS345541), IKKβ inhibitor (IMD0354) and NF-κB inhibitor (triptolide), and no effect was observed for PKC inhibitor (H7). The transcriptional activities determined from three separate transfections have been combined, and the values are expressed with SE. Significant differences from control: $^{**}P < 0.01$.

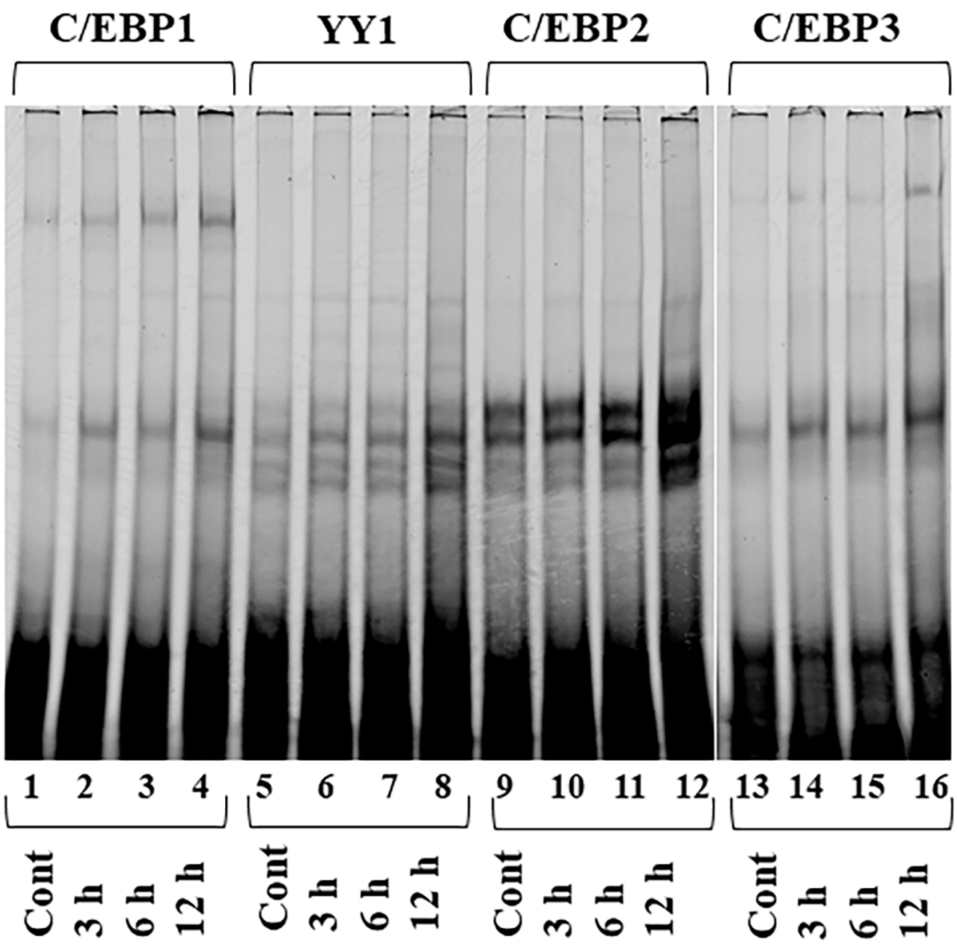


**Fig. 10** Gel mobility shift assays using C/EBP1, YY1, C/EBP2 and C/EBP3. Cy5-labeled double-stranded C/EBP1, YY1, C/EBP2 and C/EBP3 oligonucleotides were incubated with nuclear proteins obtained from Ca9-22 cells stimulated with TNF-α (10 ng/ml) for 3, 6, and 12 h. DNA-protein complexes were separated in a 6% polyacrylamide gel and scanned with Typhoon TRIO+ variable Mode Imager.

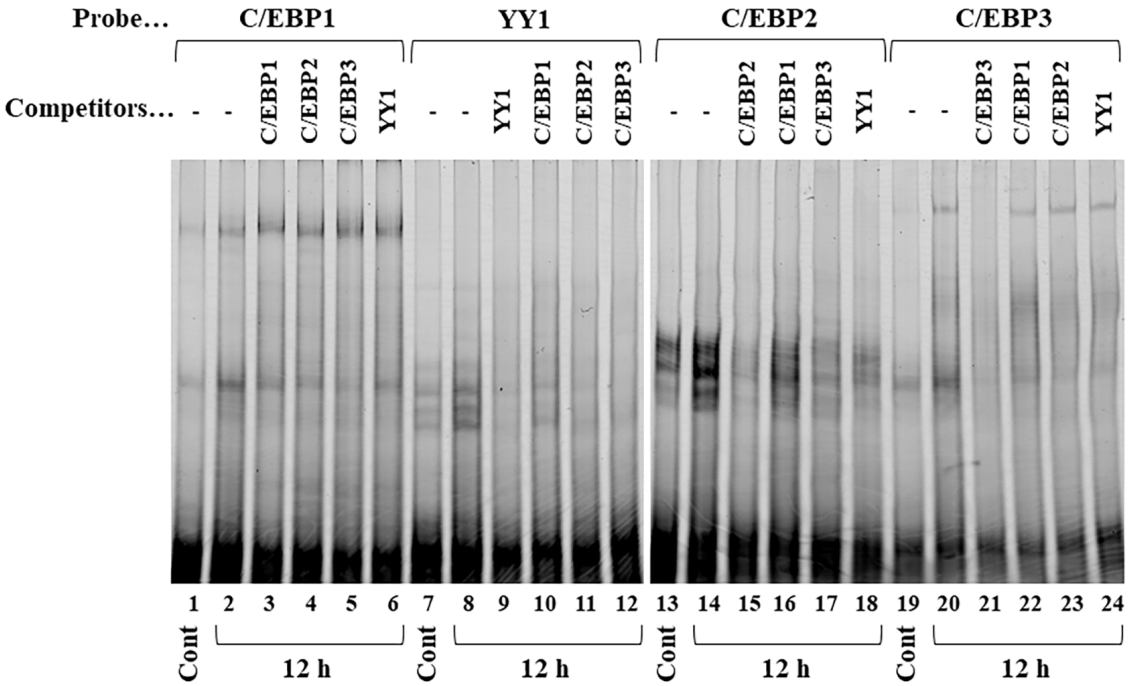


**Fig. 11** Specific binding of nuclear proteins to C/EBP1, YY1, C/EBP2 and C/EBP3. Competition assays were performed using 40-fold molar unlabeled oligonucleotides for C/EBP1, YY1, C/EBP2 and C/EBP3. DNA-protein complexes were separated in a 6% polyacrylamide gel and scanned with Typhoon TRIO+ variable Mode Imager.

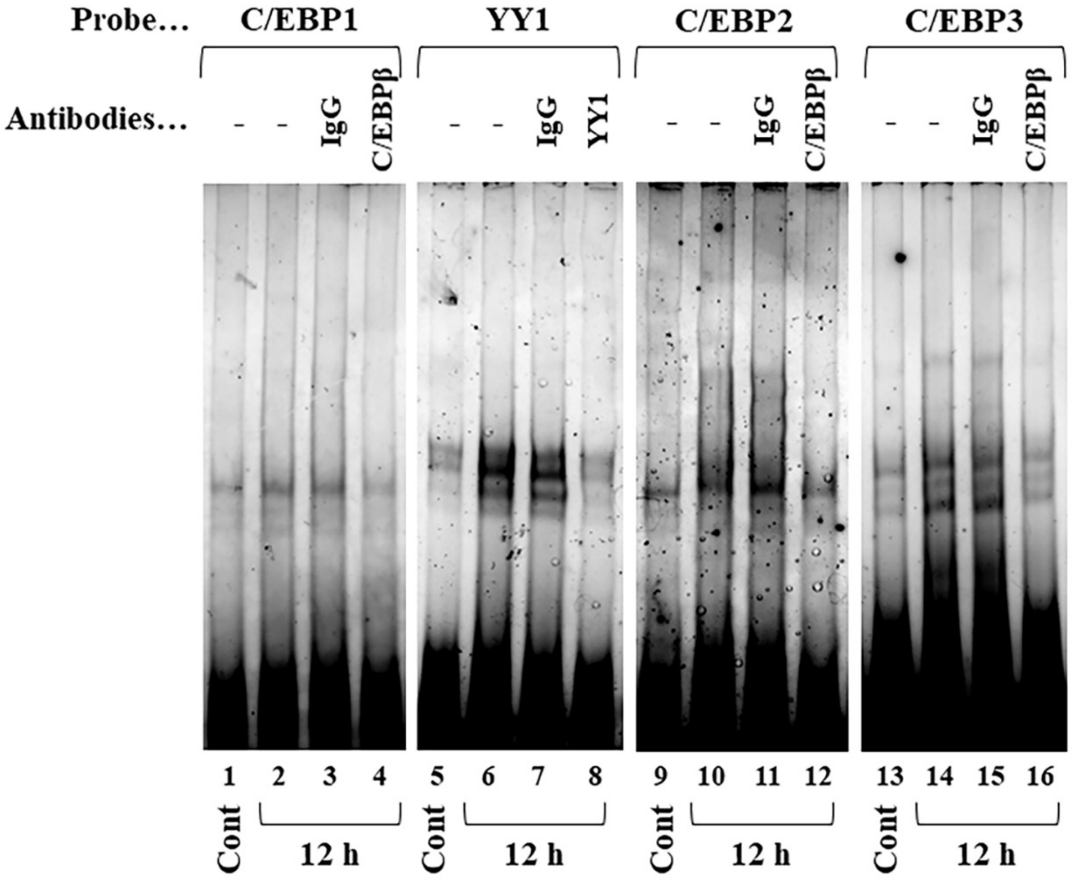


**Fig. 12** Supershift assays using antibodies to C/EBPβ and YY1. Supershift experiments were performed with 0.4 μg of antibodies against C/EBPβ and YY1 added separately to each gel shift reaction and DNA-protein complexes were separated by electrophoresis through a 6% polyacrylamide gel and scanned with ChemiDoc.

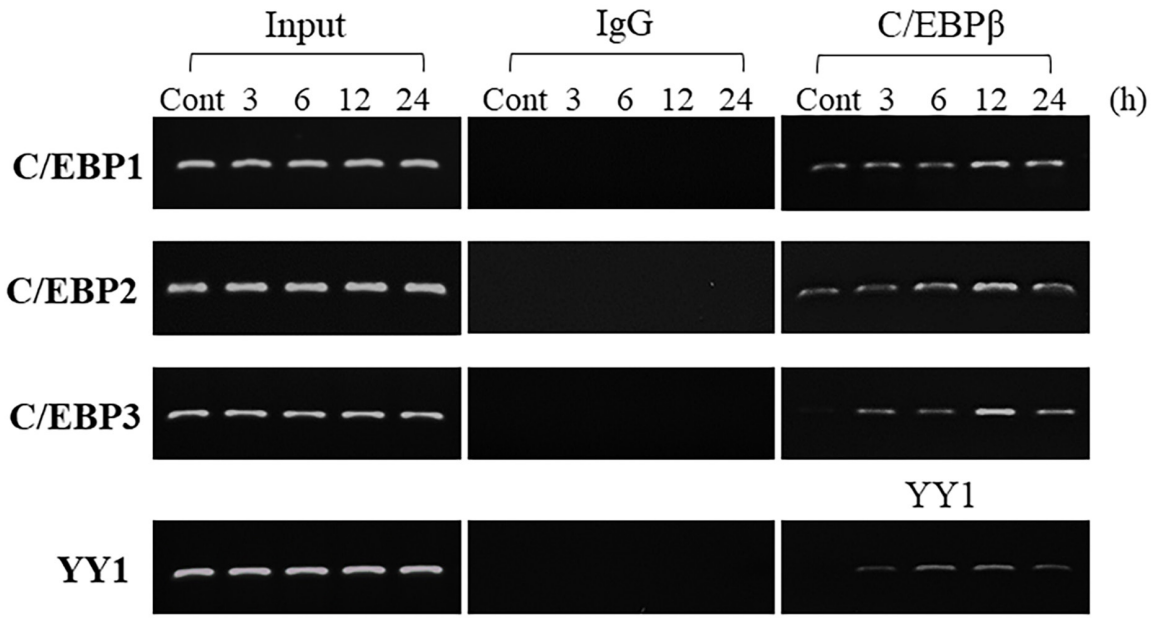


**Fig. 13** ChIP analyses of transcription factors binding to C/EBP1, YY1, C/EBP2 and C/EBP3 in the human ODAM gene promoter in Ca9-22 cells. PCR bands amplified and corresponding to DNA-protein complexes immunoprecipitated with antibodies showed that C/EBPβ and YY1 interacted with a chromatin fragment containing the C/EBP1, YY1, C/EBP2 and C/EBP3 which were increased in Ca9-22 cells following stimulation with TNF-α (10 ng/ml).

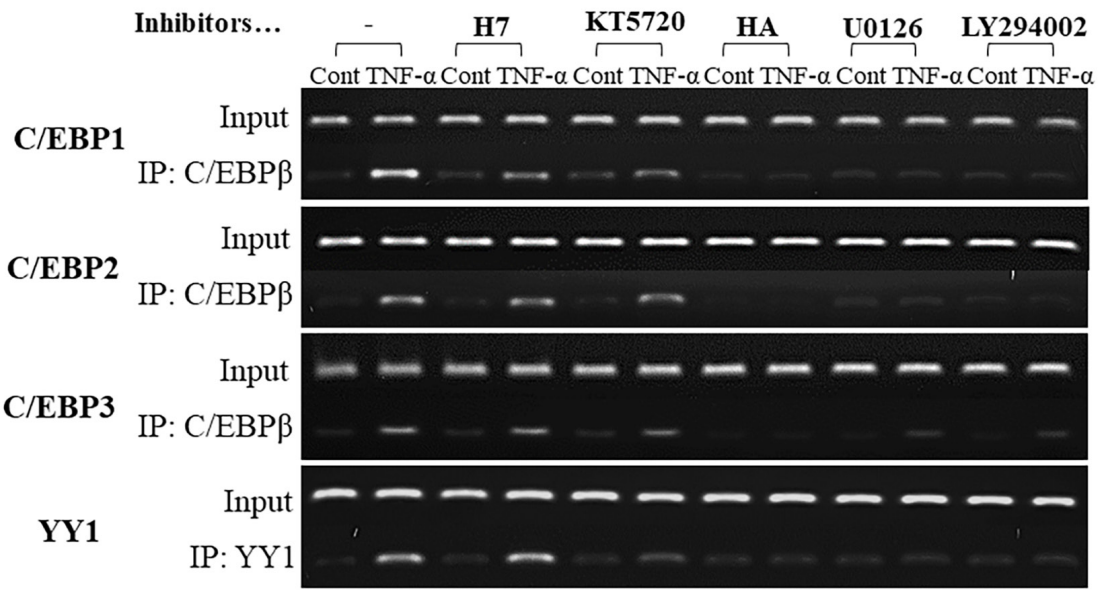


**Fig. 14** ChIP analyses of transcription factors binding to C/EBP1, YY1, C/EBP2 and C/EBP3 under the treatment by TNF-α with kinase inhibitors. Treatments of HA, U0126 and LY294002 almost completely abolished and KT5720 partially inhibited the induction of C/EBPβ and YY1 transcription factors bindings to C/EBP1, YY1, C/EBP2 and C/EBP3 by TNF-α (10 ng/ml, 12 h).